Journal of Magnetic Resonance **143,** 321–328 (2000)
doi:10.1006/jmre.1999.1995, available online at http://www.idealibrary.com on IDEAL®

Heteronuclear Local Field NMR Spectroscopy under Fast Magic-Angle Sample Spinning Conditions

Dan McElheny, Enrico DeVita, and Lucio Frydman[1]

Department of Chemistry (M/C 111), University of Illinois at Chicago, 845 West Taylor Street, Chicago, Illinois 60607-7061

Received July 13, 1999; revised December 2, 1999

The acquisition of bidimensional heteronuclear nuclear magnetic resonance local field spectra under moderately fast magic-angle spinning (MAS) conditions is discussed. It is shown both experimentally and with the aid of numerical simulations on multispin systems that when sufficiently fast MAS rates are employed, quantitative dipolar sideband patterns from directly bonded spin pairs can be acquired in the absence of ^{1}H–^{1}H multiple-pulse homonuclear decoupling even for "real" organic solids. The MAS speeds involved are well within the range of commercially available systems (10–14 kHz) and provide sidebands with sufficient intensity to enable a reliable quantification of heteronuclear dipolar couplings from methine groups. Simulations and experiments show that useful information can be extracted in this manner even from more tightly coupled –CH_2– moieties, although the agreement with the patterns simulated solely on the basis of heteronuclear interactions is not in this case as satisfactory as for methines. Preliminary applications of this simple approach to the analysis of molecular motions in solids are presented; characteristics and potential extensions of the method are also discussed.

INTRODUCTION

The measurement of site-specific anisotropic NMR coupling parameters constitutes one of the most reliable ways of elucidating the nature of motions in solids at a molecular level (*1–3*). Temperature variations in the ^{1}H linewidths and relaxation parameters of a solid sample can provide a straightforward indication of dynamics (*4*), yet molecular details can best be learned from measurements of more localized quadrupolar (e.g., ^{2}H) or dipolar (e.g., ^{1}H–^{13}C) interactions. At the center of these approaches lies the measurement of how a particular NMR anisotropy is affected by motion, followed by a quantitative analysis of these changes in terms of plausible motional models. In spite of their proven usefulness these methods face a number of technical difficulties for their accurate implementation, such as site-specific deuteration for the quadrupole measurements or the efficient use of two-dimensional (2D) rotor-synchronized homonuclear decoupling sequences for the local field determinations (*5–8*). The first of these methods is thus simple and versatile in spectroscopic terms but chemically demanding, whereas the second approach has the potential to reveal the dynamic status for several sites in the sample simultaneously and at natural abundance but must overcome challenging instrumental tune-up procedures. These difficulties did not preclude the exploitation of these methods by a growing number of research groups whose work, particularly during the past decade, has been decisive in advancing both the technology of state-of-the-art solids NMR and the promise of this spectroscopy toward the analysis of complex polymeric materials (*1–13*).

While attempting to apply these and other methods to elucidate molecular motions in synthetic aromatic polyamides and polyesters, we found that moderately fast magic-angle spinning (MAS) rates may actually enable the routine and quantitative implementation of 2D local field experiments even in the absence of homonuclear decoupling; this presentation discusses the main spectroscopic features of these observations. It was found that although slow MAS rates are insufficient for decoupling ^{1}H–^{1}H interactions and yield quantitatively inaccurate heteronuclear dipolar sideband patterns, the apparent dipolar coupling of a C–H pair converges to a reproducible and reliable value when spinning rates ν_r reach the 10- to 13-kHz range. Such ideal-like and unscaled sideband patterns were observed upon suitably processing the wide variety of methine-containing systems that we analyzed experimentally, and their behavior displayed an excellent match when compared with density matrix predictions on realistic multispin systems. By contrast to what has generally been observed when using multipulse ^{1}H–^{1}H decoupling (*12–16*), the apparent ^{13}C–^{1}H dipolar couplings resulting from these experiments tended to be slightly larger than the values predicted from diffraction bond lengths; on the basis of numerical simulations on extended spin systems this behavior could be traced to nonbonded heteronuclear couplings to distal protons. As is the case with the traditional, multiple-pulse based forms of local field spectroscopy, it was found that the sideband patterns yielded by these fast MAS experiments can clearly distinguish between static systems and a variety of dynamic cases such as flipping

[1] To whom correspondence should be addressed at Department of Chemistry (M/C 111), University of Illinois at Chicago, 845 W. Taylor Street, Room 4500, Chicago, IL 60607-7061. Fax: (312) 996-0431. E-mail: lucio@samson.chem.uic.edu.

1090-7807/00 $35.00

aromatic rings or freely rotating groups. It is noteworthy that both experiments and simulations indicate that at moderately high spinning speeds even methylenic local field sideband patterns can be analyzed in terms of pairwise H–C–H heteronuclear dipole interactions. The protocols employed in the data processing and simulation of these MAS experiments is presented, and some of their potential uses and extensions are discussed.

EXPERIMENTAL

Over the years numerous forms of 2D separate local field experiments correlating ^{13}C (or ^{15}N) chemical shifts with ^{1}H–X heteronuclear couplings have been described under static, variable-angle spinning and magic-angle spinning conditions (*6–8, 11–21*). The majority of these experiments relied on ^{1}H–^{1}H decoupling during the evolution by means of multipulse homonuclear sequences (WAHUHA, MREV-8, etc.), and incorporated rotor synchronized π-pulses for removing chemical shift effects during t_1 as well as ^{1}H-decoupling during direct X-nucleus signal acquisition. Other than for the absence of homonuclear ^{1}H–^{1}H decoupling, this is the same procedure adopted for this study (Fig. 1), which relied instead on fast MAS during indirect evolution for the removal of ^{1}H–^{1}H interactions. All of these experiments were assayed on a laboratory-built spectrometer operating at a 301.6-MHz ^{1}H frequency (75.8 MHz ^{13}C) equipped with a 4-mm doubly-tuned probe capable of spinning samples up to 18 kHz. In all cases a ramped ^{13}C cross polarization centered at ≈50-kHz fields and t_2 decoupling CW RF fields exceeding 100 kHz were used (*22*). All samples were purchased from Aldrich and used without further processing; typical 2D acquisition experiments on these compounds involved 10–16 t_1 increments equally distributed over one rotor period, 128 scans/t_1 point, 1- to 2-ms contact times, and 1.5-s recycle delays. Following the procedure discussed by Griffin, Schaefer, and others (*8, 23*), sideband spectra were obtained from the resulting dipole-encoded signals by first normalizing the amplitude-modulated rotational echo at $t_1 = 0$ and $t_1 = 1/\nu_r$ via a positive exponential multiplication $\exp(+t_1/T_2)$ and then replicating this single rotor echo signal until achieving the desired digital resolution along the indirect ν_1 dimension. The validity and consequences resulting from this renormalization/replication procedure are further discussed below.

To shed further light on this experimental protocol and its results a series of numerical simulations were also carried out employing either a magnetization-vector model applicable to isolated ^{13}C–^{1}H pairs or a full Dyson time propagation of CH_n density matrices ($n \leq 5$) incorporating the effects of both ^{13}C–^{1}H and ^{1}H–^{1}H spin–spin couplings (*24*). In order to compare simulated best fits with experimental sideband patterns, the ratios between the first few sidebands (I_1/I_0, I_2/I_0, etc.) were calculated for the actual MAS rate employed as a function of the heteronuclear dipole couplings strength, and then the dipolar coupling that best fitted the experimental results was chosen following a Herzfeld–Berger-type analysis (*25*). As is further discussed below these best fits were always computed under the assumption that no ^{1}H–^{1}H interactions were present; this assumption coupled to experimental uncertainties (evaluated on the basis of repetitive measurements) implied that in some cases a range of dipolar couplings could fit the experimental sideband data equally well. These fitting ranges are expressed in this study by error bars; usually the sideband ratios resulting from these ranges of coupling constants did not differ from the targeted sideband intensity ratios by more than 5%.

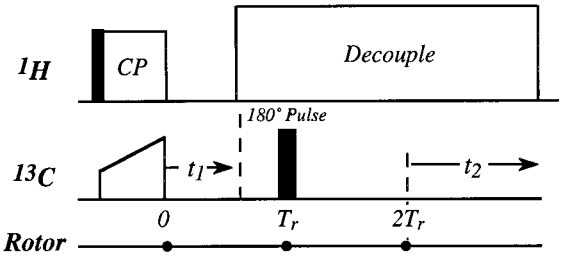

FIG. 1. 2D separate local field pulse sequence employed throughout most of the experiments discussed in this study. T_r denotes the duration of a rotor period, equal to the inverse of the MAS speed ($1/\nu_r$).

RESULTS AND DISCUSSION

As has been extensively described in the literature the 2D NMR experiment in Fig. 1 will separate along the isotropic chemical shift dimension ν_2 patterns defined by the evolution Hamiltonian,

$$\mathcal{H}(t_1) = [\sum_I \nu_{IS}(t_1) I_z] S_z + \sum_{I<J} \nu_{IJ}(t_1)(3I_zJ_z - \bar{I}\cdot\bar{J}), \quad [1]$$

where S denotes the dilute nucleus being detected, I and J are nearby protons, and both the isotropic and anisotropic chemical shift effects of S are ignored due to the rotor-synchronized π-pulse in t_1. The dipolar couplings ν_{IS}, ν_{IJ} depend on the molecular geometry and are rendered time dependent by the action of the MAS (*26*),

$$\nu_{IK}(t_1) = \sum_{m=-2}^{2} \nu_{IK}^{(m)} e^{i2\pi m \nu_r t_1}. \quad [2]$$

This time dependence implies that an exact calculation of the S-spin spectrum along ν_1 will require an explicit propagation of the density matrix,

$$\rho(t_1) = U(t_1) S_x U(t_1)^{-1}, \quad [3]$$

on the basis of the time evolution operator,

$$U(t_1) = T \exp\left[-i \int_0^{t_1} \mathcal{H}(t)dt \right]. \quad [4]$$

A powder integration of these propagated matrices followed by the Fourier transformation of their expectation value,

$$S(t_1) = \mathrm{Tr}[\rho(t_1) \cdot S_+], \quad [5]$$

will thus define the spectrum obtained in the indirect dimension.

Although only information about heteronuclear ν_{IS} couplings is generally desired from this type of signals, such insight will not be directly available from the free evolution Hamiltonian in Eq. [1] due to the effects of its noncommuting hetero- and homonuclear dipolar coupling terms. This in turn brings about the demand for a homonuclear ^{1}H–^{1}H decoupling approach, so far carried out in the form of rotor-synchronized multipulse or Lee–Goldburg irradiation and generally requiring the use of slow MAS. Alternatively, since it has long been known that fast MAS can approximate many of the decoupling functions normally entrusted to RF spin irradiation (*27, 28*), it is conceivable that quantitative ν_{IS} couplings could result by adopting such a purely mechanical procedure thereby obviating the need for CRAMPS-like sequences altogether. In fact attempts to base heteronuclear local field spectroscopy solely on MAS (ν_r = 2–5 kHz) have been reported in the literature a number of times (*14, 29*), but discrepancies between the observed and expected lineshapes were observed and blamed on either homonuclear coupling effects or spin relaxation. These discrepancies, however, are removed when faster MAS rates are used and data are processed by the renormalization/repetition of a single rotor echo signal discussed under Experimental, as exemplified in Fig. 2 using $Ca(HCO_2)_2$ as a model example. This salt represents an ensemble of relatively isolated ^{13}C–^{1}H spin pairs and has been extensively characterized both by diffraction methods and by multiple-pulse local field NMR (*16, 20, 30*). When looking at its freely decaying t_1 signals under fast MAS typical rotor echoes arising from modulations of the one-bond C–H dipolar couplings can be observed (Fig. 2, top); ^{1}H–^{1}H couplings show up mainly as an irreversible damping of the signal over multiple rotor periods. Although for this particular compound these homonuclear couplings are relatively weak and do not prevent the retrieval of a clear C–H dipolar sideband spectrum, their effects are still experimentally visible in other methines as they lead to slightly broader sidebands than centerbands. This is in qualitative agreement with the behavior recently reported for homonuclear coupled systems, for which simulations show a dominance of pairwise interactions for the sideband intensities and of three-spin interactions for the sideband lineshapes (*31, 32*). Even these minor multispin distortions, however, can largely be eliminated in the heteronuclear case by exploiting the periodic nature

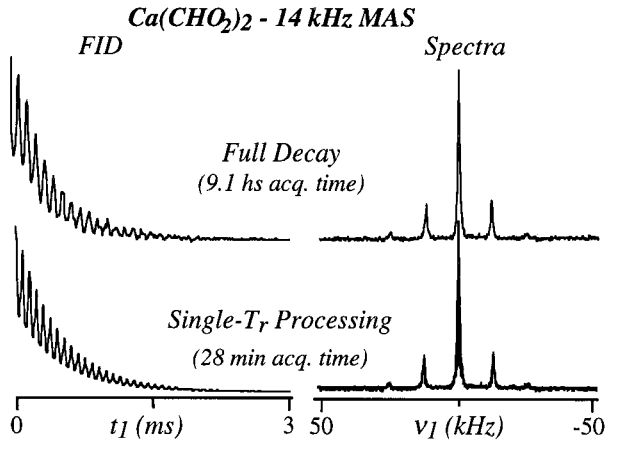

FIG. 2. Dipolar MAS patterns extracted for one of the sites in polycrystalline calcium formate. The top traces result from using a modification of the sequence in Fig. 1 which incremented t_1 over several rotor periods. The bottom data arise from using the sequence in Fig. 1 and subjecting the resulting single rotor period data to a renormalization/repetition/weighting procedure prior to obtaining the sideband spectrum. Superimposed on the latter is a best fit simulation which assumes an isolated ^{13}C–^{1}H pair with ν_{CH} = 21.8 kHz.

expected from the C–H coupling modulation and subjecting a single rotor signal to the renormalization/replication procedure. As shown at the bottom of Fig. 2, this results in a C–H dipolar sideband manifold that is virtually indistinguishable from its best fit simulation. An obvious practical advantage of this procedure is that the overall duration of the experiment is drastically reduced, with a much smaller number of t_1 increments becoming necessary.

A practical concern affecting this procedure relates to the definition of "fast" MAS rates, i.e., to the spinning speeds required for obtaining undistorted, pairwise-like heteronuclear sideband patterns. Also important to consider is the structural reliability of the couplings resulting from these fast MAS experiments. We have investigated these issues both experimentally and with the aid of numerical spin simulations. Figure 3, for instance, illustrates the spinning speed dependencies observed for the MAS dipolar patterns obtained from the two sites in calcium formate upon processing single rotor period signals and compares these traces with best fit simulations based on isolated ^{13}C–^{1}H pairs undergoing MAS. Besides the obvious effects that changing the rotor spinning speed introduces on the relative positions and intensities of the various sidebands, these simulations reveal an apparent dependence of the one-bond coupling constants characterizing the experimental traces on the rate of sample spinning: the dipolar couplings that best fit the spectra increase with ν_r and eventually level off to a final value only as ν_r reaches or exceeds 12 kHz. A qualitatively similar behavior was observed for all of the organic methine systems that were analyzed for this study (Fig. 4). This behavior agrees well with previous observations according to which smaller than expected ^{13}C–^{1}H couplings result when local field MAS experiments are carried out in the

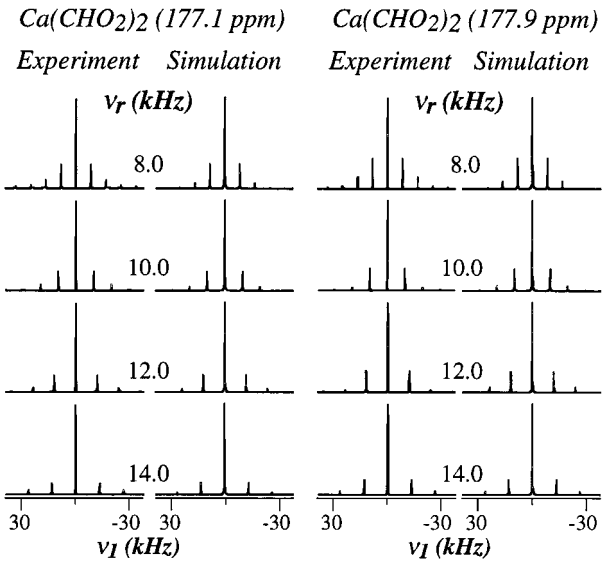

FIG. 3. Comparison between the dipolar sideband patterns obtained by processing single-T_r $Ca(CHO_2)_2$ ^{13}C NMR data acquired at different spinning rates and the best fit simulation of each spectrum obtained under the assumption of isolated ^{13}C–^{1}H spin pairs. The actual dipolar couplings employed in obtaining each of these simulations are graphed in the top left of Fig. 4.

absence of homonuclear ^{1}H–^{1}H decoupling using what is nowadays considered slow spinning conditions (1–5 kHz) (*33*). From a quantitative point of view, it is important to remark upon the close agreement between the C–H distances obtained on fitting these fast MAS $Ca(CHO_2)_2$ data (1.12 ± 0.01 and 1.16 ± 0.01 Å) and those arising from previous multiple-pulse VAS experiments (1.126 and 1.130 Å, respectively; refs. *16, 20*. Also interesting to note is the fact that the spinning speeds required for obtaining these limiting values of C–H dipolar couplings are well within current technologies even when dealing with solids possessing much denser ^{1}H–^{1}H coupling networks than $Ca(HCO_2)_2$.

To shed further insight into the validity of using the limiting values of this fast MAS protocol for recovering individual ^{13}C–^{1}H dipolar couplings, a series of multispin numerical simulations based on Eqs. [1]–[5] were carried out. Such calculations, which have the important advantage of an *a priori* knowledge of the dipolar couplings that one intends to extract, were carried out on model ^{13}C–$^{1}H_5$ systems possessing either typical aliphatic or aromatic geometries and were subsequently compared with the predictions expected from ideal, isolated ^{13}C–^{1}H pairs undergoing MAS. Representative results obtained from these variable-speed multispin calculations are illustrated in Fig. 5. A comparison between the spectra that arise by Fourier transforming a complete free evolution time-domain signal (left-hand column) with traces arising from the renormalization/repetition of single rotor echo signals (center column) confirms that the main effect introduced by the latter protocol is to remove most "nonidealities" arising from the presence of homonuclear interactions. These undesired ^{1}H–^{1}H effects appear in the ^{13}C lineshapes as powder broadenings which affect the outer sidebands more strongly than the centerband and thereby preclude a reliable quantification based on fitting the individual peaks heights. By contrast the single-T_r multispin data yield sideband patterns that, as in the case of all of the experiments, can be fitted well by simulations of a single ^{13}C–^{1}H pair, provided that its coupling constant is allowed to increase slightly with the spinning rate (Fig. 6). It is satisfying to note that, as is observed experimentally, both aromatic and aliphatic simulations predict a leveling off of the apparent couplings when spinning rates reach the 10- to 13-kHz range. These calculations do not actually clarify the origin of the attenuation in heteronuclear couplings observed under slow MAS, but these are likely to originate in residual homonuclear ^{1}H–^{1}H couplings which can reduce the apparent one-bond heteronuclear couplings via spin-diffusion-like effects (*8, 34*). Also interesting to note is the fact that, according to the CH_n multispin numerical simulations, the limiting coupling values observed under fast MAS conditions may end up exceeding the actual coupling strength derived from the single-bond ^{13}C–^{1}H distance. This trend is in contrast to what is usually observed in CRAMPS-based separate local field experiments and is apparently a consequence of small—but not negligible—distal ^{13}C–^{1}H interactions between nonbonded pairs.

Although such nonlocal dipolar contributions might limit the accuracy with which ^{13}C–^{1}H distances are determined, they

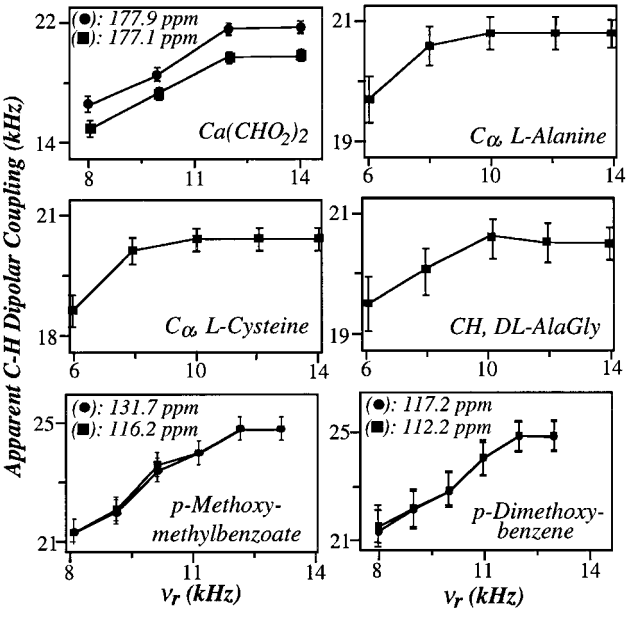

FIG. 4. Apparent spinning speed dependencies observed for the C–H dipolar couplings of the indicated methine sites, obtained upon processing single-T_r 2D MAS local field NMR data for the corresponding compounds. All couplings were obtained following the procedure indicated in Fig. 3 for the case of $Ca(CHO_2)_2$; error bars indicate the couplings' confidence limits as judged by repetitive experiments and the quality of their fits. The limiting coupling values indicate r_{CH} = 1.145 ± 0.010 Å for the C_α aminoacid carbons and r_{CH} = 1.075 ± 0.008 Å for the aromatic methines.

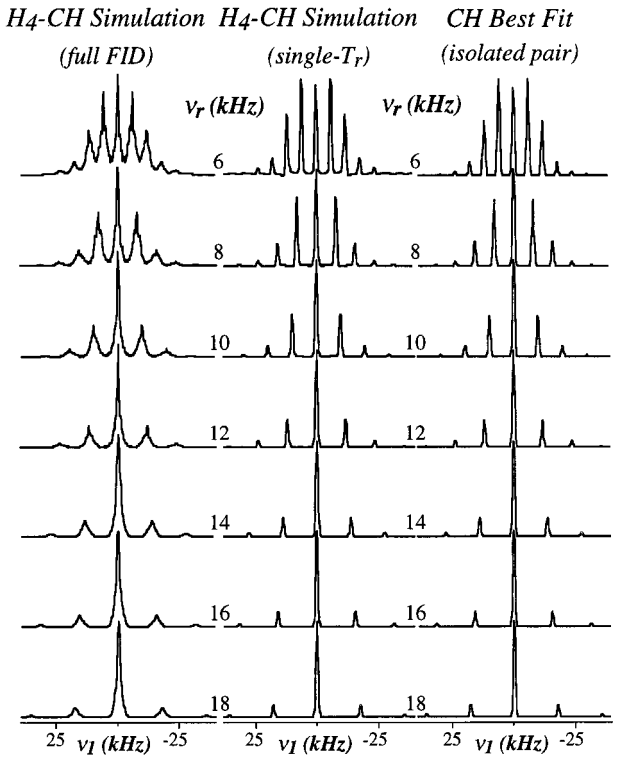

FIG. 5. ^{13}C separate local field spectra expected from a methine group inserted in a model $-^{12}CH_2-^{13}CH-^{12}CH_2-$ fragment with aliphatic geometry undergoing MAS at the indicated spinning rates. Traces on the left arise from Fourier transforming the free time evolution of the ^{13}C spin over 13 rotor periods, considering 30^3 different powder orientations, 9-μs time increments, and the Hamiltonian in Eq. [1]. The center column presents the spectra arising on subjecting the first rotor period of such propagated spin evolution data to a renormalization/repetition procedure like the one used for processing the experimental results. The right-hand column shows the best fits of these single-T_r data to spectra arising from isolated heteronuclear spin pair undergoing MAS; the individual $^{13}C-^{1}H$ couplings employed in these simulations are summarized on the right in Fig. 6.

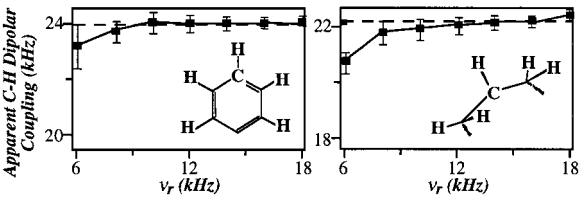

FIG. 6. Spinning rate dependencies characterizing the heteronuclear couplings of methine groups inserted in the indicated structures, obtained by fitting single rotor period multispin data as described in Fig. 5. Brackets indicate the ranges of dipolar couplings for which fits of comparable qualities could be obtained. The dashed lines indicate the actual one-bond $^{13}C-^{1}H$ couplings used in simulating the multispin data, corresponding to C–H distances of 1.085 and 1.112 Å for the aromatic and aliphatic structures, respectively. In both cases these dipolar couplings are exceeded by the limiting values arising from the best fits of the dipolar sideband spectra.

pose few complications toward the characterization of molecular dynamics on the basis of the experimental sideband patterns. Figure 7 illustrates this sensitivity of fast MAS local field to dynamics with a comparison between the experimental sideband pattern observed for a static C–H aromatic spin pair and those arising from aromatic spin pairs undergoing fast 180° flips about the phenyl's *para* axis and rapid reorientations about a high ($\geq C_3$) symmetry axis. Because all of these dynamic cases are taking place in the fast exchange regime (*4*), reproduction of the experimental data can be obtained simply by considering ideal, isolated $^{13}C-^{1}H$ spin pairs whose dipolar tensors have been averaged to new principal values by the dynamics (*2, 35*). In principle, however, there are no reasons for preventing such an approach from being applicable over other dynamic regimes with the aid of suitable $^{13}C-^{1}H$ MAS lineshape calculations.

Finally, it is worth addressing the possibility of extending these fast MAS experiments to the analysis of local ^{13}C fields in the case of methylene groups. It would be natural to assume that such results would be qualitative at best due to the strong homonuclear coupling present within the moiety, comparable to the heteronuclear interactions and unlikely to be averaged out at MAS rates which still leave meaningful C–H sidebands to be measured. Although multispin simulations do indeed show significant effects from geminal $^{1}H-^{1}H$ couplings even at moderately high MAS rates (Fig. 8), these can to a large extent be removed by subjecting the first rotor echo within this train to a renormalization/repetition procedure as described earlier. The resulting traces can then be mimicked by simulations arising from $-CH_2-$ groups which are free from internal homonuclear couplings, even though the match between these simplified calculations and the multispin-based predictions is not as perfect as in the methine cases. Moreover, even at the highest spinning rates these best fit heteronuclear simulations underestimate the individual $^{13}C-^{1}H$ couplings by about 4%. Again, the overall behavior shown by these theoretical predic-

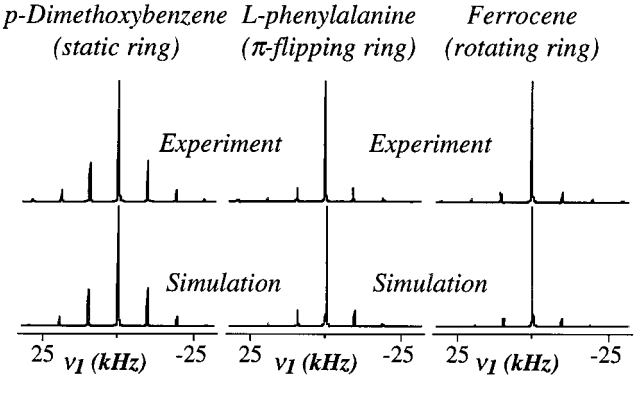

FIG. 7. Sensitivity of MAS local field sideband patterns to solid-state molecular motions. All data were collected at room temperature and $\nu_r = 10$ kHz; the slices shown were extracted from the 2D results obtained on the indicated compounds at 117.2 ppm (left), 129.0 ppm (center), and 63.1 ppm (right) and processed as described in the text. Simulations were obtained based on isolated C–H pairs separated by 1.085 Å and assumed either static (left) or exchange-averaged dipolar tensors.

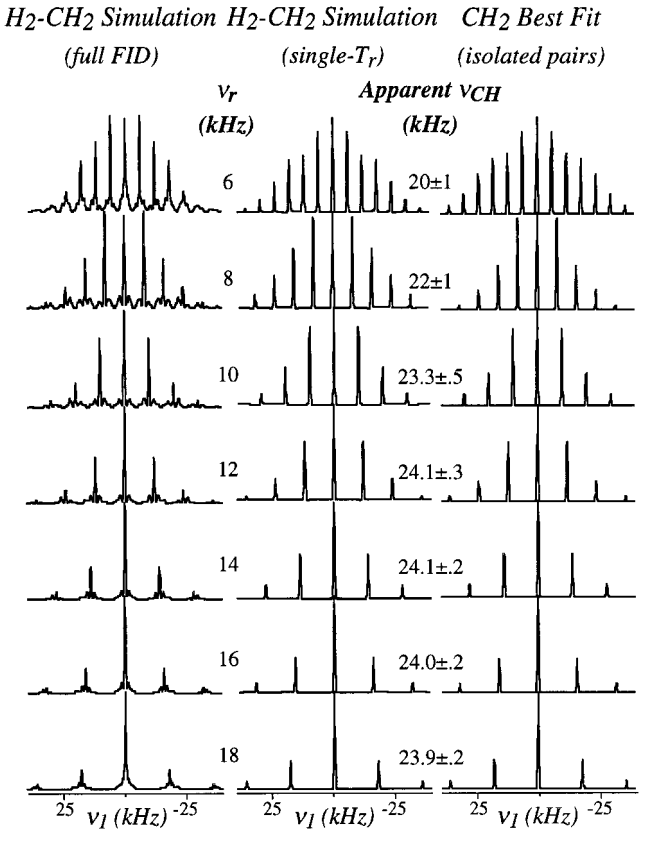

FIG. 8. Comparison between the ^{13}C local field spectra arising from a model $H^{12}C–^{13}CH_2–^{12}CH$ fragment with aliphatic geometry undergoing MAS at the indicated rates (left and center columns) versus data expected from an isolated methylene group free from homonuclear $^1H–^1H$ couplings (right). In all cases bond angles of 109.5° and C–H distances of 1.086 Å (ν_{CH} = 24.02 kHz) were assumed. The left spectra considered the full decay of the local field MAS signal over 30^3 powder orientations. The center traces arise from processing the first rotor echo of these signals as described in the text; the right spectra are the best fit of the former assuming no $^1H–^1H$ interactions. The $^{13}C–^1H$ dipolar couplings employed in these fits are indicated and their ranges denote heteronuclear one-bond couplings values that afforded spectral matchings of nearly equal quality.

tions is in very good agreement with the features that are observed experimentally for a number of different compounds (Fig. 9). Although the fits resulting from these data fail to display the steady, converging behavior that at higher spinning rates was displayed by the methines (Fig. 10), they still provide $^{13}C–^1H$ distances to within 0.02–0.03 Å accuracy thanks to the inverse cubic dependence relating geometries with coupling values. Also interesting to note is the fact that all of the analyzed methylene groups exhibited dipolar couplings in the neighborhood of what could have been expected on the basis of ideal aliphatic C–H distances (≈1.14 Å) except for L-methionine, whose ^{13}C local field spectra revealed substantially smaller heteronuclear couplings than the rest. This is likely another manifestation of the experiment's spectral sensitivity to the presence of motional dynamics, most likely reflecting methionine's conformational variability in the solid state (*37*).

CONCLUSIONS

The present work explored both theoretically and experimentally the possibility of employing moderately fast MAS techniques for measuring heteronuclear couplings within directly bonded spin systems. As did other recent NMR investigations (*38–40*), such efforts represent an attempt to exploit ongoing developments in sample spinning technologies for achieving results that hitherto demanded the use of homonuclear decoupling sequences. Pursuing such an avenue may not only simplify the execution and analysis of NMR experiments but also, by lifting the demand on slow spinning speeds, open up the sensitivity and resolution bonuses that result from high-field fast MAS operation. Judging from the local field results and simulations described in this work, replacing spin- by spatial-space averaging of homonuclear couplings appears entirely feasible in organic solid applications once MAS rates begin to exceed 10–12 kHz. It does not, however, appear desirable to exceed these moderate speeds by a large margin as beyond ca. 18 kHz heteronuclear interactions will have been largely averaged away and little information will remain in the sidebands; on the other hand, much of the quantitative accuracy of the experiment is lost if ν_r drops below 7–8 kHz.

Besides the potential of these fast MAS local field experiments for structural determinations, the main applications of these methods can be expected to center on motional studies of solids. In terms of experimental simplicity and spectral features this approach yields information that is comparable with that available from ^1H wideline separation methods (*2, 41*), even if its quantitative interpretation in terms of dynamic models is aided by the better defined nature of heteronuclear interactions. When faced with alternative solid-state dynamic NMR approaches fast local field MAS spectroscopy compares favorably in experimental simplicity, ease of interpretation, and lack of synthetic labeling demands. These goals, however, are achieved at the expense of a significant sacrifice in spectral information content as the use of fast MAS limits the coupling information to only three or four sideband intensity ratios. Nevertheless, the fact that the experiment can be focused on measuring just a few points within the $0 \leq t_1 \leq 1/\nu_r$ interval endows it with the possibility of achieving high S/N in short acquisition times and therefore with a high reliability (*42*). Furthermore, since at the relatively high spinning speeds which are employed both calculations and experiments indicate that the single rotor ^{13}C spin evolution is determined by well-defined heteronuclear dipolar couplings, alternative routes could be explored to enhance the information afforded by this experiment. We have found, for instance, that simple π-pulse manipulations can be used to multiply in a simple manner the effective coupling constants defining the C–H dipolar manifolds (*43*), thereby bringing a substantial increase into the intensities of the outer sidebands. Also worth considering are simple data acquisition and processing alternatives involving the Fourier transformation of a single (renormalized) rotor

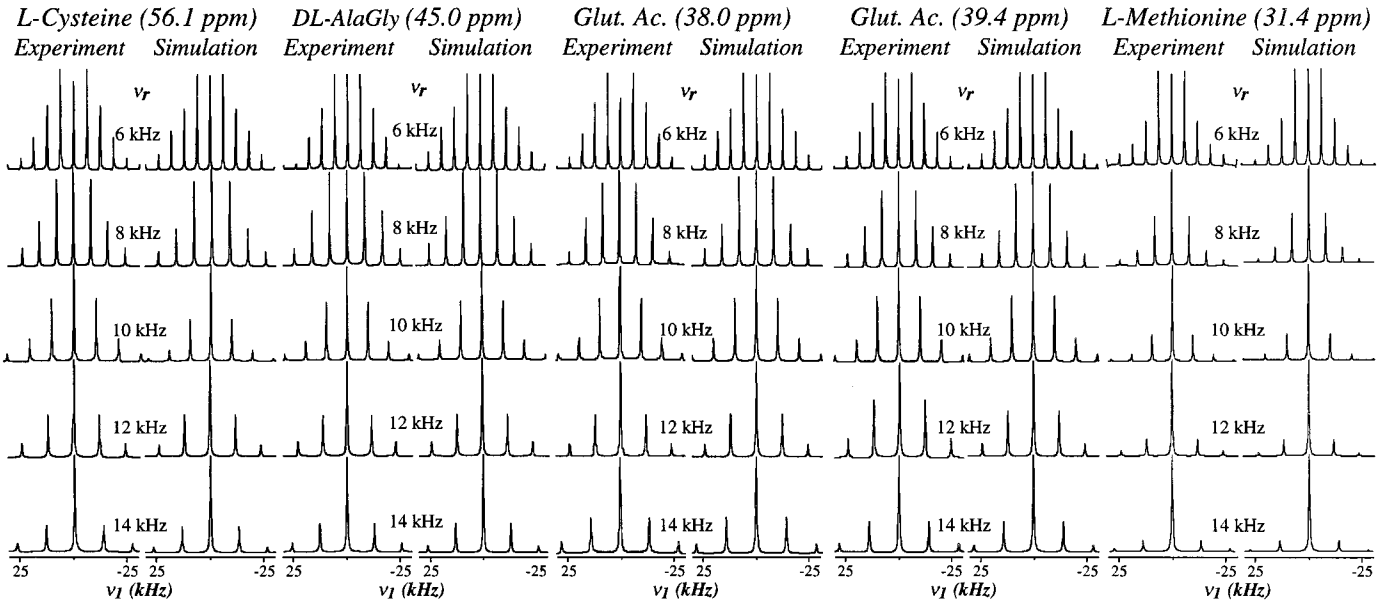

FIG. 9. Comparison between the local field dipolar sideband patterns obtained by processing single-T_r data from the indicated methylenic ^{13}C resonances and best fit simulations calculated under the assumption of isolated $-CH_2-$ groups with 109.5° H–C–H angles, C_2 symmetry, and no ^1H–^1H interactions. The dipolar ^{13}C–^1H couplings used to simulate each of these spectra are summarized in the graphs of Fig. 10.

echo and constant-time schemes that do not require renormalization and thus enable a reduction of the observations to only half a rotor period. Some of these routes are currently being explored.

ACKNOWLEDGMENTS

This work was supported by the National Science Foundation through Grants DMR-9806810 and CHE-9841790 (Creativity Extension Award). L.F. is a Camille Dreyfus Teacher–Scholar (1996–2001), University of Illinois Junior Scholar (1997–2000), and Alfred P. Sloan Fellow (1997–2000).

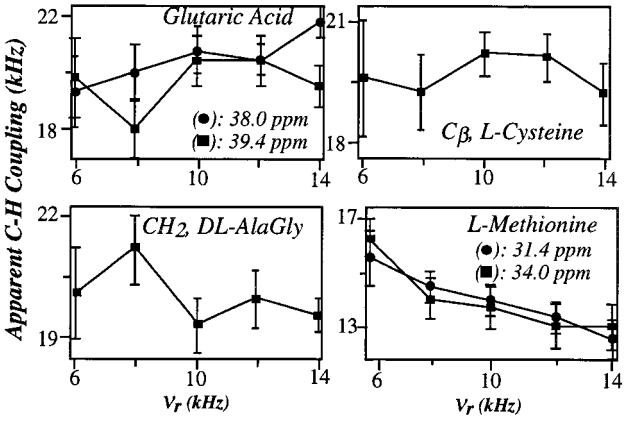

FIG. 10. Spinning speed dependencies obtained for the apparent one-bond C–H couplings of the indicated methylene sites from the MAS local field simulations in Fig. 9. The monotonic drop observed for the couplings in L-methionine could originate in a slight heating of the sample with increasing spinning rates (*36*).

REFERENCES

1. V. J. McBrierty and K. J. Packer, "Nuclear Magnetic Resonance in Solid Polymers," Cambridge Univ. Press, Cambridge (1993).
2. K. Schmidt-Rohr and H. W. Spiess, "Multidimensional Solid-State NMR and Polymers," Academic Press, New York (1994).
3. F. A. Bovey and P. A. Mirau, "NMR of Polymers," Academic Press, San Diego (1996).
4. C. A. Fyfe, "Solid State NMR for Chemists," CFC Press, Ontario (1983).
5. H. W. Spiess, *Adv. Polym. Sci.* **66,** 23, (1985).
6. M. G. Munowitz, R. G. Griffin, G. Bodenhausen, and T. H. Wang, *J. Am. Chem. Soc.* **103,** 2529, (1981).
7. M. G. Munowitz and R. G. Griffin, *J. Chem. Phys.* **76,** 2848, (1982).
8. J. Schaefer, R. A. McKay, E. O. Stejskal, and W. T. Dixon, *J. Magn. Reson.* **52,** 123, (1983).
9. H. W. Spiess, *Chem. Rev.* **91,** 1321 (1991).
10. J. Wendoloski, K. Gardner, J. Hirschinger, H. Miura, and A. English, *Science* **247,** 431, (1990).
11. J. Schaefer, E. O. Stejskal, R. A. McKay, and W. T. Dixon, *Macromolecules* **17,** 1479 (1984).
12. J. Schaefer, M. D. Sefcik, E. O. Stejskal, R. A. McKay, W. T. Dixon, and R. E. Cais, *Macromolecules* 17, (1984).
13. M. Poliks and J. Schaefer, *Macromolecules* **23,** 3426 (1990).
14. J. E. Roberts, G. S. Harbison, M. G. Munowitz, J. Herzfeld, and R. G. Griffin, *J. Am. Chem. Soc.* **109,** 4163 (1987).
15. G. G. Webb and K. W. Zilm, *J. Am. Chem. Soc.* **111,** 2455 (1989).
16. T. Nakai, J. Ashida, and T. Terao, *Mol. Phys.* **67,** 839 (1989).
17. M. E. Stoll, A. J. Vega, and R. W. Vaughn, *J. Chem. Phys.* **65,** 4093 (1976).
18. J. S. Opella and J. S. Waugh, *J. Chem. Phys.* **66,** 4919 (1977).

19. M. Linder, A. Hohener, and R. R. Ernst, *J. Chem. Phys.* **73,** 4959 (1980).

20. T. Nakai, J. Ashida, and T. Terao, *J. Chem. Phys.* **88,** 6049 (1988).

21. B. M. Fung, J. Afzal, T. L. Foss, and M. Chan, *J. Chem. Phys.* **85,** 4808 (1986).

22. O. B. Peersen, X. Wu, I. Kustanovich, and S. O. Smith, *J. Magn. Reson. A* **104,** 334 (1993).

23. M. Hong, J. D. Gross, and R. G. Griffin, *J. Phys. Chem. B* **101,** 5869 (1997).

24. U. Haeberlen, "High Resolution NMR in Solids," Academic Press, New York, (1976).

25. J. Herzfeld and A. E. Berger, *J. Chem. Phys.* **73,** 6021 (1980).

26. M. M. Maricq and J. S. Waugh, *J. Chem. Phys.* **70,** 3300 (1979).

27. E. R. Andrew, A. Bradbury, and R. G. Eades, *Nature* **182,** 1659 (1958).

28. I. J. Lowe, *Phys. Rev. Lett.* **2,** 285 (1959).

29. P. Palmas, P. Tekely, and D. Canet, *Solid State NMR* **4,** 105 (1995).

30. N. Burger, H. Fuess, and S. A. Mason, *Acta Crystallogr. Sect. B* **33,** 1968 (1977).

31. S. Ray, E. Vinogradov, G.-J. Boender, and S. Vega, *J. Magn. Reson.* **135,** 418 (1998).

32. C. Filipu, S. Hafner, J. Schnell, D. E. Demco, and H. W. Spiess, *J. Chem. Phys.* **110,** 423 (1999).

33. J. Schaefer, personal communication.

34. G. Sinning, M. Mehring, and A. Pines, *Chem. Phys. Lett.* **43,** 382 (1976).

35. M. Mehring, "High Resolution NMR in Solids," Second ed., Springer-Verlag, Berlin (1983).

36. A. R. Grimmer, A. Kretschmer, and V. B. Cajipe, *Magn. Reson. Chem.* **35,** 86 (1997).

37. L. E. Diaz, F. Morin, C. L. Mayne, D. M. Grant, and C.-J. Chang, *Magn. Reson. Chem.* **24,** 167 (1986).

38. A. Mehta, B. Trounge, S. Burns, X. Wu, I. Wu, and K. W. Zilm, "38th Rocky Mountain Conference," Poster 315, Denver, CO (1996).

39. S. Hafner and H. W. Spiess, *Concepts Magn. Reson.* **10,** 99 (1998).

40. P. K. Isbester, J. L. Brandt, T. A. Kestner, and E. J. Manson, *Macromolecules* **31,** 8192 (1998).

41. N. Zumbulyadis, *Phys. Rev. B* **33,** 6495 (1986).

42. P. Hodgkinson and L. Emsley, *J. Chem. Phys.* **107,** 4808 (1997).

43. M. Hong, J. D. Gross, C. M. Rienstra, R. G. Griffin, K. K. Kumashiro, and K. Schmidt-Rohr, *J. Magn. Reson.* **129,** 85 (1997).